Colloid Polym Sci (2008) 286:647–654
DOI 10.1007/s00396-007-1806-6

ORIGINAL CONTRIBUTION

Study on line tension of air/hexadecane/aqueous surfactant system

Youichi Takata · Hiroki Matsubara · Takashi Matsuda · Yoshimori Kikuchi · Takanori Takiue · Bruce Law · Makoto Aratono

Received: 17 April 2007 / Revised: 17 November 2007 / Accepted: 17 November 2007 / Published online: 10 December 2007

Abstract We measured the line tension of the air/hexadecane/aqueous solution of the dodecyltrimethylammonium bromide (DTAB) system as a function of the molality of DTAB aqueous solution at 298.15 K. The experimental values of the line tension were 10^{-10} to 10^{-12} N, and they coincided with the theoretical estimates. Furthermore, it was found that the line tension changes in sign from positive to negative at around 0.750 mmol kg^{-1}. This concentration is close to the point of transition from partial to frustrated-complete wetting. Taking into account the profiles of the free energy of the air/water surface, previously developed by Indekeu to understand the interrelationship between the wetting transition and line tension, it is suggested that the sign reversal of the line tension can be attributed to the transition from partial to frustrated-complete wetting.

Y. Takata · H. Matsubara · T. Matsuda · Y. Kikuchi · T. Takiue · M. Aratono
Department of Chemistry and Physics of Condensed Matter, Graduate School of Sciences, Kyushu University, Fukuoka 812-8581, Japan

B. Law
Condensed Matter Laboratory, Department of Physics, Kansas State University, Manhattan, KS 66506-2601, USA

Present address:
Y. Takata (✉)
Faculty of Pharmaceutical Sciences and Institute of Colloid and Interface Science, Tokyo University of Science, 2641 Yamazaki, Noda, Chiba 278-8510, Japan
e-mail: yoichit@rs.noda.tus.ac.jp

Keywords Line tension · Wetting transition · Phase transition in adsorbed film · Free-energy profile

Introduction

In three-phase systems such as fluid/liquid/liquid or fluid/liquid/solid, there exists a contact line where the three interfaces meet. A kind of tension acts on the three-phase contact line, which is analogous to the interfacial tension acting on the interface between two bulk phases. This tension is known as "line tension." Since the introduction of the concept of line tension by Gibbs [1], its study has gradually expanded considering both the experimental and theoretical viewpoints. Line tension plays an important role in microscopic systems and has therefore attracted a considerable amount of attention these days. This is because the systems that have been considered by the researchers have been increasingly miniaturized. Based on this background, the studies on line tension consider various topics from the fundamentals (e.g., heterogeneous nucleation [2, 3], foam films [4]) to applications (e.g., domain line tension at the liquid/liquid interface [5, 6], biological systems like vesicles [7], or bilayer membranes [8]). In this sense, a full-scale investigation of line tension would be an area of significant current interest.

Line tension has been measured by many researchers using various techniques [9–17]. For example, Langmuir [9] calculated the linear tension of a liquid alkane lens on water surface and the effect of insoluble monolayers on it from the force balance at the edge of the liquid lens. Mingins and Scheludko [10] observed the attachment of small glass particles to the air/water surface from the inside of a pendant drop. Then, they estimated the value of line tension, ~10^{-11} N, by considering a balance between the

force of gravity acting on the particle and the energy barrier for the formation of a three-phase contact line. Neumann's research group extensively conducted the measurement of the liquid-drop-size dependence of the contact angle on a solid substrate, which is one of the most feasible systems. They obtained a positive line tension of the order of 10^{-6} N [11, 12, 14]. Pompe et al. [15] employed the tapping mode of atomic force microscopy to determine the contact angle from the height images of a microdroplet placed on a solid surface. This experiment yielded a value of $\sim 10^{-10}$ N for the line tension.

Despite such experimental researches, results that were quite different from the theoretical estimates were often reported. These differences may have partly originated from the usage of an air/liquid/*solid* system instead of an air/liquid/*liquid* system. As pointed out by some authors [18–20], it is very difficult to prepare a molecularly smooth solid surface, and therefore, the hysteresis of the contact angle due to the heterogeneity and/or roughness of the solid surface possibly affects the line tension. Recently, this problem is being resolved theoretically by considering the effect of the surface roughness on the line tension [21]. As mentioned elsewhere [22] on one hand, the line tension (or line energy) associated with the pinning effects due to the solid surface imperfections effectively reduces with a decrease in the Young's equilibrium contact angle. Based on this fact, some experiments [23–25] conducted on the solid surfaces provided the line tension of the expected order in a regime of very low contact angles (e.g., near the wetting transition). However, it is indispensable to perform experiments on molecularly smooth liquid surfaces to elucidate the nature of line tension. A few investigations have been conducted on the line tension of fluid systems in the past. Aveyard et al. [26] succeeded in measuring the line tension of the air/dodecane/water system. They determined the radius and dihedral angle of a dodecane droplet by interferometry and then estimated the value of line tension with the aid of the Neumann–Young equation (Eq. 1). As a result, they obtained a line tension of the order of 10^{-11} N, which was in good agreement with the theoretical estimates [27].

In addition to the above-mentioned controversial experimental results of line tension, there are also difficulties in theoretical studies because the treatment of line-tension phenomena is complicated by the presence of three bulk phases as well as three interfaces in the vicinity of the three-phase contact line. The representative theoretical studies on line tension, which were based on local theories, were performed by Widom's group [28, 29]. Subsequently, these studies were extended to a more quantitative theory, which included the non-local features, by Getta and Dietrich [30] and Bauer and Dietrich [31]. Furthermore, by focusing on the wetting transition, Indekeu [32] and Dobbs [33] successfully explained the theoretical connection between the line tension and the wetting behavior of the three-phase systems. The wetting phenomena have been considered as among the most interesting behaviors observed in three-phase systems. Therefore, they have been investigated experimentally in various types of systems [34–37] and regarded as good candidates for both theoretical and experimental studies on line tension.

From the viewpoint of the states of interfacial films, we have investigated the wetting behavior of the hexadecane phase on the aqueous solution of ionic surfactants [38–40]. At the air/water surface in these systems, the states of adsorbed film of a surfactant change discontinuously from a lower film density [like a three-dimensional (3-D) gas phase] to a higher one (like a 3-D liquid phase) at a certain concentration of aqueous surfactant solution. We have also found that this phenomenon, known as the phase transition in the adsorbed film, induces the wetting transition of the hexadecane phase on the aqueous solution. From the fact that the hexadecane droplet was still observed after the wetting transition, furthermore, it was suggested that the wetting transition in these systems is the one from *partial* to *frustrated-complete* wetting, which means the coexistence of the hexadecane droplet with its thin film [41]. These results are of interest in the respect that we can measure the line tensions accompanied by the wetting transition. Therefore, we measured the line tension as a function of the surfactant concentration in the aqueous solution. The results have already been published in a concise manner [42]. The aim of this study is to first describe the details of the experiments and results and then closely examine the change in the line tension with surfactant concentration by considering Indekeu's [32] theory on the basis of the free-energy profiles of the air/water surface established in our previous studies [43].

Experimental

Materials

n-Hexadecane (Kanto Chemical) was distilled fractionally under reduced pressure. Its boiling point was 407.15 K at 1.4 mmHg. The purity of *n*-hexadecane was confirmed by the value of its interfacial tension with water at 298.15 K under atmospheric pressure and also by the absence of the time dependence of its interfacial tension. Dodecyltrimethylammonium bromide (DTAB, Tokyo Kasei Kogyo) was purified twice by recrystallization from a mixture of acetone and ethanol. No minimum was observed in the surface tension vs molality of the DTAB aqueous solution curves around the critical micelle concentration. Water was

distilled three times: the second and third steps were carried out by using dilute alkaline permanganate solution.

Apparatus for line-tension measurement

The experimental setup is almost the same as that employed by Aveyard et al. [26], as depicted schematically in Fig. 1. We ensured that the temperature of the whole system was maintained constant throughout the measurement procedure and that the three phases were mutually saturated among each other for strictly maintaining the equilibrium state. The former was achieved by placing the entire apparatus, including the microscope and charge-coupled device (CCD) camera, in an air thermostat as well as by circulating temperature-regulated water around the glass cell. For the latter, oil and aqueous surfactant solution phases were mutually saturated in advance, and also the narrow apertures were sealed with the oil to prevent the water and oil phases from vaporizing. The temperature of the system was regulated within 298.15±0.1 K.

We employed a BX60F Microscope and LMPlan FL 20× BD Reflectance Objective with a working distance of 12 mm (Olympus Optical). Monochromatic light (Hg line at 546 nm), for illumination, was directed from a mercury lamp via an interference filter. The lens images observed by a digital monochrome CCD Camera CS3330 (Tokyo Electronic) mounted on the microscope were saved in a Digital Still Recorder DKR-700 (Sony). These images were processed and analyzed using the Scion Image program (Scion) to acquire the intensity data. Finally, the intensity profile of the droplet fringes was fitted to the theoretical curves using Excel to simultaneously determine the dihedral angle and lens radius.

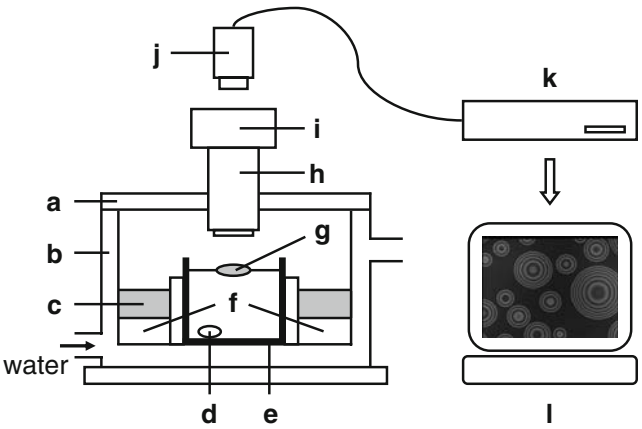

Fig. 1 Illustration of experimental set up: (*a*) glass lid; (*b*) thermostat; (*c*) oil reservoir; (*d*) magnetic rotor; (*e*) glass cell; (*f*) aqueous phase; (*g*) oil droplet; (*h*) microscope objective; (*i*) microscope; (*j*) CCD camera; (*k*) MD recorder; (*l*) personal computer

In this study, the suitable size of droplet lenses was 10–100 μm. The lenses were prepared by stirring a larger lens, placed onto the water surface, for 30 min. The images of the lenses were recorded every 1 h up to 3 h after stirring. The dihedral angle was dependent on lens radius, but the dependency did not change with the period after the stirring beyond the accuracy of the measurement.

Principle of line-tension estimation

When an oil droplet stably exists at the air/water surface (Fig. 2) and the two angles α and β are very small as in this system, Aveyard et al. [26] derived the following relation:

$$y = \gamma^{\mathrm{AO}} \cos\left(\frac{\gamma^{\mathrm{OW}}\delta}{\gamma^{\mathrm{AO}}+\gamma^{\mathrm{OW}}}\right) + \gamma^{\mathrm{OW}} \cos\left(\frac{\gamma^{\mathrm{AO}}\delta}{\gamma^{\mathrm{AO}}+\gamma^{\mathrm{OW}}}\right) = \gamma^{\mathrm{AW}} - \frac{\tau}{r}, \tag{1}$$

where the dihedral angle $\delta = \alpha + \beta$ Thus, the slope of a straight line drawn from the plots of the left-hand side of Eq. 1 against r^{-1} yields the line tension τ. The γ^{AO} and γ^{OW} values were measured by the pendant drop method with an accuracy of ±0.05 mN m^{-1} [39]. The δ and r values were simultaneously estimated by interferometry, as shown by Aveyard et al. [26]. The intensity of reflected light is described as a function of α, β, and r, and the dihedral angle δ $(= \alpha + \beta)$ and lens radius r are then determined by fitting a theoretical interference profile for a set of α, β, and r to the experimental one observed by using a microscope. In the fitting procedure, some attenuation in the intensity profile occurs while moving away from the center of the lens (Fig. 3). Therefore, we carefully considered the number of peaks and the relative intensity of each point obtained from both theoretical and experimental interference profiles; this procedure differs from the least squares method adopted by Aveyard et al. [26]. The accuracies of δ

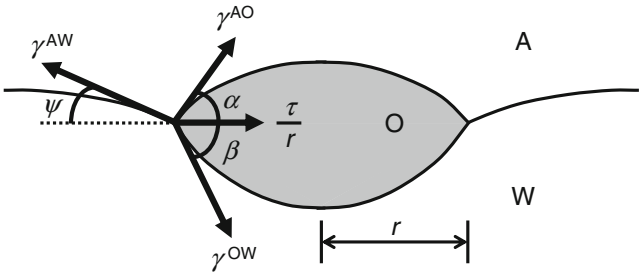

Fig. 2 Schematic illustration of an oil droplet (*O*) floating on the air/water (*A*/*W*) interface; γ^{ab} interfacial tension of the α/β interface; α (β, ψ) angle between the A/O (O/W, A/W) interface and the plane containing the three-phase contact line; r lens radius; τ line tension

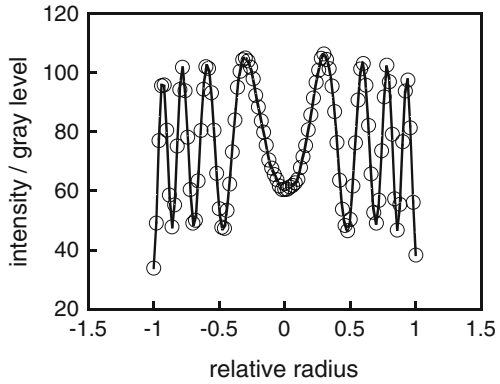

Fig. 3 Plots of intensity of reflected light against the relative radius

and r values obtained by our method are ±0.01 degree and ±0.6452 μm, respectively.

Results and discussion

Line-tension measurement in the DTAB system

The dihedral angles and lens radii of the air/hexadecane/aqueous solution of the DTAB system were measured at nine different concentrations of aqueous solution, and all the data were fitted to Eq. 1. The representative plots of the left-hand side of Eq. 1 against r^{-1} at 0.505 and 1.013 mmol kg^{-1} have already been shown in our previous paper [42], and the line tensions evaluated from the best-fit line are summarized in Table 1. It should be noted that the order of line tension is within 10^{-10} to 10^{-12} N and coincides well with the theoretical estimates. Here, the line tension was obtained by re-examining the fitting process reported previously in [42], where we took into account that the fitting exhibited a rather larger scatter with an increase in the dihedral angle, and the line tension in this paper is marginally different from that in [42]. This shows that there is still room for improvement in line-tension estimation; however, the consideration of its sign, described below, remains unchanged.

Table 1 Values of the line tension at various concentrations of the DTAB system

Molality (mmol kg^{-1})	Line tension (10^{-12} N)
0.505	+30.7
0.677	+13.9
0.699	+13.0
0.734	+3.20
0.797	−3.40
0.912	−55.1
1.013	−17.1
1.037	−34.5
1.106	−117

The more important point is, as shown in Table 1 and Fig. 3 in our previous paper [42], that the line tension decreases gradually with an increase in the surfactant concentration and changes its sign from positive to negative at around 0.750 mmol kg^{-1}. The reversal of the sign was also supported by the phenomenological observation that smaller lenses gradually disappeared, and the larger ones increased with time at 0.505 mmol kg^{-1}; on the other hand, the larger lenses tended to split into smaller lenses at 1.013 mmol kg^{-1} (Fig. 4 in [42]). Because the line tension is regarded as a type of free energy for forming a unit length of the three-phase contact line, a positive line tension is expected to bring about lens coalescence to minimize the total line length (similar to Ostwald ripening in a three-dimensional system). If the line tension is negative, it would cause the break up or fission of large lenses into smaller ones (to increase the total line length). Thus, the phenomenological observation of the clear change from coalescence to fission at around 0.750 mmol kg^{-1} is consistent with the change in the sign of the line tension around this surfactant concentration. Toshev et al. [3] reported a similar dependence of the line tension for a black film system with an increase in the salt concentration and claimed that the line tension changed from positive to negative in a continuous manner. This continuous change in the line tension could be the result of their films always remaining in the Newton black film regime and never undergoing a transition between a common black film and a Newton black film [44] in the range of salt concentration considered.

Theoretical considerations regarding the sign of the line tension

In our previous studies on the wetting behavior of hexadecane lens onto the DTAB aqueous solution surface, the transition from partial to frustrated-complete wetting was observed at around 0.6 mmol kg^{-1} [39, 40]. Here, from a theoretical point of view, we demonstrate that the transition from positive to negative line tension can be attributable to this wetting transition.

In 1992, Indekeu [32] developed the theory of line tension from various aspects of wetting based on de Gennes' [45] review. According to his theory, the force acting through the thin film connected to the lens displaces the lens profile near the three-phase contact line from the idealized one that obeys the Young–Laplace equation to the actual one, as schematically shown in Fig. 4. The excess free energy required for this deforma-

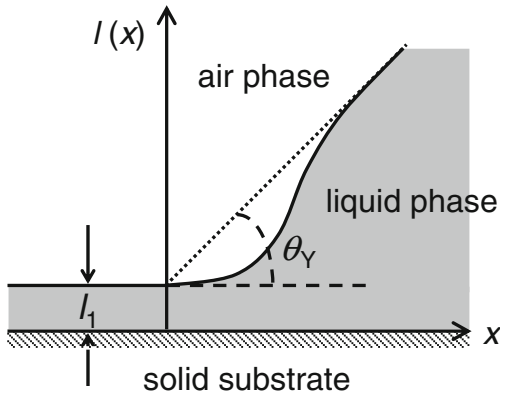

Fig. 4 Idealized (*dotted line*) and actual (*solid line*) profiles near the three-phase contact line. θ_Y shows the Young's contact angle. The liquid lens is in equilibrium with a film of the thickness l_1

tion is the line tension. Thus, the line tension is considered to be the following functional [32]:

$$\tau[l] = \int_{-\infty}^{\infty} \left[\frac{\gamma}{2} \left(\frac{dl}{dx} \right)^2 + V(l) + \text{const.} \right] dx, \tag{2}$$

where γ is the surface tension, l the interface displacement which is a function of x, and $V(l)$ the interface potential. The first term in the integrand of Eq. 2 is attributable to the increase in the interfacial area, while the second term is attributable to the free energy per unit area when a uniform film of thickness l is present. By minimizing Eq. 2 and taking the potential at $l \to \infty$, which corresponds to the sum of the air/oil and oil/water interfacial tensions, as a reference state, the following equation for the line tension can be derived [32]:

$$\tau = (2\gamma)^{1/2} \xi \int_{l_1}^{\infty} \left[V(l)^{1/2} - S^{1/2} \right] dl, \tag{3}$$

where ξ is the bulk correlation length, l_1 the film thickness in equilibrium with a drop, and S the spreading coefficient. This equation suggests that the equilibrium line tension is calculated by estimating the interface potential $V(l)$ and integrating Eq. 3 from the thickness l_1 to infinity.

Next, we need to estimate the interface potential corresponding to the free energy per unit area of the air/water surface. Referring to our recent theoretical study [43], the interface potential was determined as follows. The free energy of the air/water surface consists of two parts: one is a short-range contribution, which means the surface tension of a mixed monolayer composed of surfactant and oil molecules, and the other is a long-range one, which means van der Waals interaction acting through the oil phase. The former is estimated by applying a lattice model to the mixed monolayer at the air/water surface, in which there are Γ_m adsorption sites occupied by surfactant molecules with probability x_s and by oil molecules with probability x_o. In conclusion, the following equation for the air/water surface tension γ^{AW} was obtained: [43]

$$\begin{aligned} \gamma^{AW} = \gamma_0^{AW} + kT\Gamma_m \Bigg[& -2x_s \ln \frac{m}{K_L} - 6x_o + \frac{1}{2kT} \\ & \left(x_s^2 \beta_{ss} + x_o^2 \beta_{oo} + 2x_o x_s \beta_{os} \right) + 2x_s \ln x_s \\ & + x_o \ln x_o + (1 - x_s - x_o) \ln (1 - x_s - x_o) \\ & + (1 - x_s) \ln (1 - x_s) \Bigg] \end{aligned} \tag{4}$$

Here, γ_0^{AW} represents the surface tension of pure water, K_L the Langmuir constant, and β_{ij} the interaction parameter between i and j molecules, respectively. From Eq. 4, we can calculate the value of γ^{AW} as a function of the fraction x_o occupied by oil molecules. On the other hand, the long-range part was expressed by van der Waals interaction using the Hamaker constant A [46]

$$U(l) = -\frac{A}{12\pi l^2}, \tag{5}$$

where l is the sum of the thickness of a mixed monolayer and oil layer on it. In this system, we assumed that the dielectric property of a mixed monolayer is equal to that of oil phase. Then, the combination of short-range (Eq. 4) and long-range (Eq. 5) interactions yields the interface potential.

Figure 5 shows the interface potential as a function of the layer thickness at five concentrations of DTAB aqueous solution. Here, taking into account that the thickness of oil layer in the frustrated-complete wetting regime provided an almost constant value of ~0.7 nm from ellipsometry [40], we employed a short-range interaction in the regime of $l<$ 0.7 nm, whereas a long-range interaction in the regime of $l>$0.7 nm. There are two minima in these profiles except for Fig. 5e: one is at nearly zero thickness, and the other is at l=0.7 nm. At the primary minimum, the total coverage ($=x_s+x_o$) of the air/water surface by surfactant and oil molecules is about 5% from the theoretical calculation, and thus, we can say that a very dilute monolayer is formed there. At the secondary minimum, on the other hand, the total coverage goes up to ~97%, and therefore, it is said that the air/water surface is almost occupied by surfactant and oil molecules. Let us look more closely at the variation of the interface potential with increasing the concentration of DTAB aqueous solution. At a low DTAB concentration (Fig. 5a), the energy of the primary

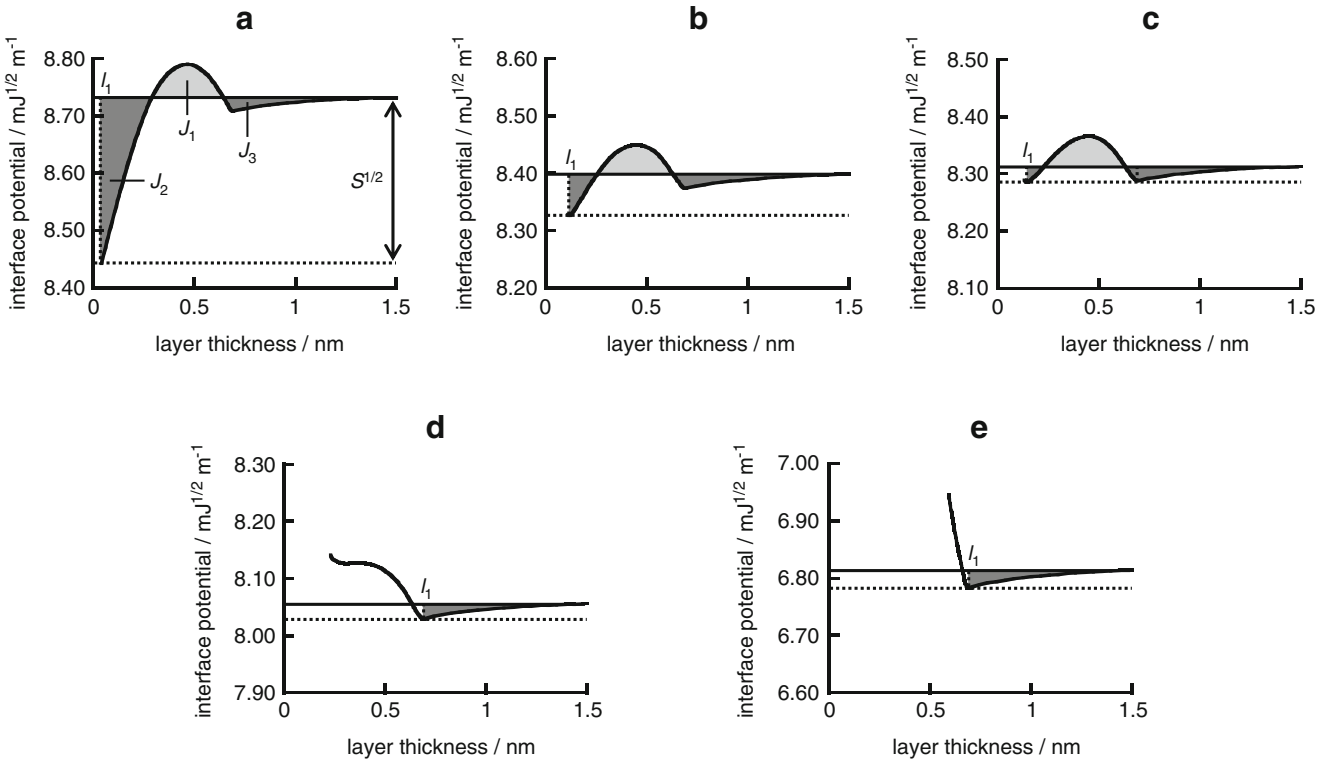

Fig. 5 Interface potential profile associated with the transition from partial to frustrated-complete wetting from [43] **a** 0.2 mmol kg^{-1} and **b** 0.7 mmol kg^{-1} in partial wetting regime; **c** 0.87 mmol kg^{-1} at the point of the wetting transition; **d** 1.5 mmol kg^{-1} and **e** 8.0 mmol kg^{-1} in frustrated-complete wetting regime. In the frustrated-complete wetting regime, a drop is in equilibrium with a film of thickness l_1~0.7 nm

minimum is lower than that of the secondary minimum, which implies that the partial wetting state is thermodynamically stable. The energy of these two minima approaches each other with an increase in the DTAB concentration, (Fig. 5b) and they become equal to each other at the wetting transition point (Fig. 5c). Beyond this point, the secondary minimum is more stable (Fig. 5d), and consequently, the frustrated-complete wetting state is obtained (Fig. 5e). Thus, the line tension changes discontinuously at the wetting transition point due to the facts that the initial spreading coefficient is positive around the wetting transition point, there are two minima below and at the wetting transition point at which they have equal values, and then there exists only one minimum in the frustrated-complete wetting regime.

Based on such energy profiles, let us apply Indekeu's theory to our system.

The sign of the line tension is dependent on the difference between the positive (J_1) and negative (J_2 and J_3) contributions to the integral of Eq. 3. It should be noted that the lower limit l_1 in Eq. 3 refers to the film thickness in equilibrium with a hexadecane lens. Thus, we can understand the behavior of the line tension associated with the transition between the *partial* and *frustrated-complete wetting*. Although the difference in the integrals, $J_1-J_2-J_3$, can be either positive or negative, depending on the shape of the interface potential, it will take a positive value just below the DTAB concentration at which the wetting transition occurs, according to the interface potential shown in Fig. 5b. In the frustrated-complete wetting regime, on the other hand, the film thickness in equilibrium with a hexadecane drop is the one at the secondary minimum, and therefore the line tension should be negative, as shown in Fig. 5d, e. Thus, we have demonstrated that the line tension is positive at the DTAB concentrations, which are lower than the wetting transition point, and negative at the DTAB concentrations, which are higher than the wetting transition point. Furthermore, according to this theory, there will be a discontinuous change in the line tension from a positive to negative value at the wetting transition point of our system (Fig. 5c). This result differs from the experimental results for black film systems [3] and complete wetting systems [19, 23–25].

Here, it would be instructive to mention the relation between Dobbs' theory [33] and the present results of line tension. The Dobbs' theory indicates a discontinuous change of $7\sim8\times10^{-12}$ N in the line tension from a positive

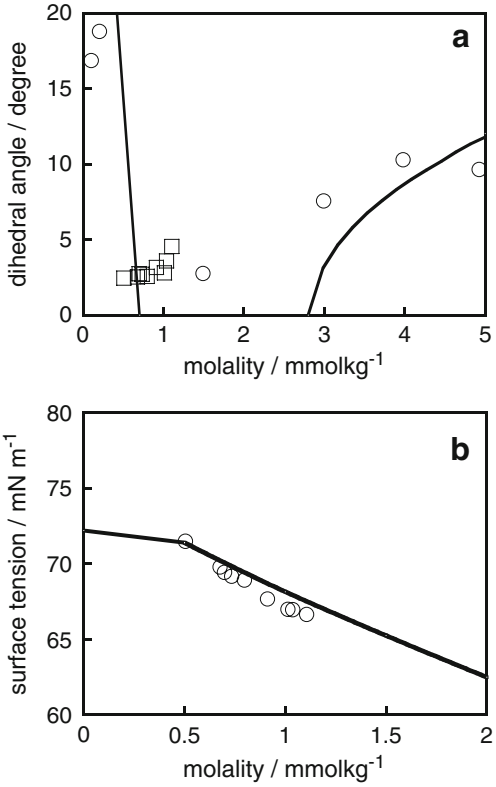

Fig. 6 **a** Plots of dihedral angles obtained from drop-shape analysis (*circle*) and from interferometry (*square*) against the molality of DTAB aqueous solution. The *solid line* shows the dihedral angles calculated from the equilibrium interfacial tensions by using Eq. 5 in [39]. **b** Plots of air/water surface tension obtained from interferometry against the molality of DTAB aqueous solution. The *solid line* shows the surface tension vs molality of DTAB aqueous solution curve measured by the surface tensiometry (Fig. 1 in [39])

to negative value at the thin–thick transition point. As mentioned above, the interface potential in Fig. 5 also suggests that the discontinuous change in sign of the line tension associated with the transition between *partial* and *frustrated-complete wetting*. However, since the error in our experiments was much larger than the theoretically expected discontinuous change of $7\sim8\times10^{-12}$ N, we understand that the apparently continuous change in line tension observed in this study certainly corresponds to the thin–thick transition shown in Fig. 3 of [33]. Another interesting point in relation to the comparison of Dobbs' theory with the experiments is the behavior of line tension at a very low surfactant concentration below the wetting transition point because the theory and Fig. 5a show that the line tension may change its sign also at a low concentration. Unfortunately, the present experimental method is not accessible to this low concentration region because of rather large dihedral angles [26, 42].

Thus far, we have studied lenses of microscopic size, of the order of tens to hundreds of microns, in which the line tension plays an important role. Here, let us examine the limiting values of the dihedral angles, δ_∞, and air/water surface tensions, γ_∞^{AW}, determined for the microscopic system when the size of the lens is increased to a macroscopic size (greater than a millimeter). The δ_∞ values determined by extrapolating the δ vs r^{-1} curves up to $r^{-1}=0$ are plotted against the molality of DTAB aqueous solution (squares) in Fig. 6a and compared with the dihedral angles θ_O measured previously by the drop shape analysis of macroscopic hexadecane lens (circles) [39]. It seems that the δ_∞ values slightly differ from the θ_O values even when the experimental error in θ_O (at most ±1.2 degree) is taken into account. In a similar manner, the γ_∞^{AW} value (circles) is estimated from the intercept of the y vs r^{-1} curves (Fig. 2 in [42]) given by Eq. 1 and compared with the γ^{AW} values obtained from interfacial tensiometry (solid line) [39] in Fig. 6b. Again, we observed that a small difference exists between the values of surface tension.

Now, let us infer the origin of such differences, which should inherently agree with each other in the limit of $r \to \infty$ because of negligibly small line-tension effect. The important point may be that we have to consider two kinds of radii of oil droplet, i.e., the lens radius, r, and the radius of curvature of the air/oil and oil/water interfaces, R^{AO} and R^{OW}. Here, the following equation

$$r = R^{AO}\sin\alpha = R^{OW}\sin\beta \tag{6}$$

holds. Taking account of very small dihedral angles as in this system, $R \to \infty$ as $r \to \infty$. Therefore, the γ_∞^{AW} value inevitably indicates the air/water surface tension obtained under the condition of $R \to \infty$ as well as $r \to \infty$. On the other hand, it has been previously demonstrated that the air/water surface tension in the presence of an oil droplet depends on the internal pressure of oil phase, that is, the radius of curvature R, as shown by Eq. 76 of [47]. Accordingly, there is a possibility that the γ^{AW} values, which were obtained experimentally by the pendant-drop technique, provide the air/water surface tension at a certain R, rather than $R \to \infty$. Thus, a small difference between the values of surface tension may be brought by such different condition. From the fact that the equilibrium-spreading coefficient S_∞ calculated by using the γ_∞^{AW} values becomes negative over the DTAB concentration studied, it is concluded that we need the value of S_∞ to describe the wetting behavior accurately.

Acknowledgement YT acknowledges the support from the Japan Society for the Promotion of Science (JSPS) through the Grant-in-Aid for JSPS Fellows. This work was also supported by the Grant-in-Aid for Exploratory Research (number 17655062) from JSPS. BL acknowledges the partial support for this work from the US National Science Foundation (grant number DMR-0603144).

References

1. Gibbs JW (1961) The scientific papers of J. Willard Gibbs. Dover, New York
2. Scheludko A, Chakarov V, Toshev B (1981) J Colloid Interface Sci 82:83–92
3. Toshev BV, Platikanov D, Scheludko A (1988) Langmuir 4:489–499
4. Ivanov IB, Kralchevsky PA, Dimitrov AS, Nikolov AD (1992) Adv Colloid Interface Sci 39:77–101
5. Li M, Tikhonov AM, Schlossman ML (2002) Europhys Lett 58:80–86
6. Tikhonov AM, Pingali SV, Schlossman ML (2004) J Chem Phys 120:11822–11838
7. Umeda T, Suezaki Y, Takiguchi K, Hotani H (2005) Phys Rev E 71:011913
8. Harden JL, MacKintosh FC, Olmsted PD (2005) Phys Rev E 72:011903
9. Lamgmuir I (1933) J Chem Phys 1:756–776
10. Mingins J, Scheludko A (1979) J Chem Soc Faraday Trans 75:1–6
11. Gaydos J, Neumann AW (1987) J Colloid Interface Sci 120:76–86
12. Li D, Neumann AW (1990) Colloids Surf 43:195–206
13. Dussaud A, Vignes-Adler M (1997) Langmuir 13:581–589
14. Amirfazli A, Kwok DY, Gaydos J, Neumann AW (1998) J Colloid Interface Sci 205:1–11
15. Pompe T, Fery A, Herminghaus S (1998) Langmuir 14:2585–2588
16. Stockelhuber KW, Radoev B, Schulze HJ (1999) Colloids Surf A 156:323–333
17. Faraudo J, Bresme F (2003) J Chem Phys 118:6518–6528
18. Chen P, Susnar SS, Amirfazli A, Mak C, Neumann AW (1997) Langmuir 13:3035–3042
19. Wang JY, Betelu S, Law BM (2001) Phys Rev E 63:031601
20. Checco A, Guenoun P, Daillant J (2003) Phys Rev Lett 91:186101
21. Lin FYH, Li D, Neumann AW (1993) J Colloid Interface Sci 159:86–95
22. Tadmor R (2004) Langmuir 20:7659–7664
23. Wang JY, Betelu S, Law BM (1999) Phys Rev Lett 83:3677–3680
24. Pompe T, Herminghaus S (2000) Phys Rev Lett 85:1930–1933
25. Pompe T (2002) Phys Rev Lett 89:076102
26. Aveyard R, Clint JH, Nees D, Paunov V (1999) Colloids Surf A 146:95–111
27. Rowlinson JS, Widom B (1982) Molecular theory of capillarity, chapter 8. Oxford University Press, Oxford New York
28. Widom B, Clarke AS (1990) Physica A 168:149–159
29. Widom B, Widom H (1991) Physica A 173:72–110
30. Getta T, Dietrich S (1998) Phys Rev E 57:655–671
31. Bauer C, Dietrich S (1999) Euro Phys J B 10:767–779
32. Indekeu JO (1992) Physica A 183:439–461
33. Dobbs H (1999) Langmuir 15:2586–2591
34. Aratono M, Kahlweit M (1991) J Chem Phys 95:8578–8583
35. Chen LJ, Yan WJ (1993) J Chem Phys 98:4830–4837
36. Ragil K, Meunier J, Broseta D, Indekeu JO, Bonn D (1996) Phys Rev Lett 77:1532–1535
37. Pfohl T, Riegler H (1999) Phys Rev Lett 82:783–786
38. Aratono M, Kawagoe H, Toyomasu T, Ikeda N, Takiue T, Matsubara H (2001) Langmuir 17:7344–7349
39. Matsubara H, Ikeda N, Takiue T, Aratono M, Bain CD (2003) Langmuir 19:2249–2253
40. Wilkinson KM, Bain CD, Matsubara H, Aratono M (2005) ChemPhysChem 6:547–555
41. Bertrand E, Dobbs H, Broseta D, Indekeu J, Bonn D, Meunier J (2000) Phys Rev Lett 85:1282–1285
42. Takata Y, Matsubara H, Kikuchi Y, Ikeda N, Matsuda T, Takiue T, Aratono M (2005) Langmuir 21:8594–8596
43. Matsubara H, Aratono M, Wilkinson K, Bain CD (2006) Langmuir 22:982–988
44. Adamson AW, Gast AP (1997) Physical chemistry of surfaces, chapter 14. Wiley, New York
45. de Gennes PG (1985) Rev Mod Phys 57:827–863
46. Israelachvili JN (1985) Intermolecular and surface forces, chapter 11. Academic, London
47. Aratono M, Toyomasu T, Ikeda N, Takiue T (1999) J Colloid Interface Sci 218:412–422